AIVC 11616

BUILDING AND ENVIRONMENT

PERGAMON

Building and Environment 34 (1999) 329–333

Deflection of wall-jets in ventilated enclosures described by pressure distribution

M. T. Karimipanah*

Centre for Built Environment, Royal Institute of Technology, Box 88, S-801 02, Gävle, Sweden

Received 2 September 1997; revised 3 December 1997; accepted 20 May 1998

Abstract

The pressure field in fluid systems reflects the flow configuration. Measurements of the pressure along the perimeter of a slot ventilated room have been conducted for different room sizes. The momentum of the jet at the end of the room is decreased with increasing room length. The impingement region (region where the influence of the opposing wall is present) starts, independent of room size, when the distance from the supply device is about 70% of the room length. Corner flows could not be predicted by CFD using the linear eddy viscosity or standard stress models. However, these effects may be captured by using a second moment closure turbulence model with a new near wall approach now available in literature.

Nomenclature

b height of the inlet slot (m)
H height of room (m)
L length of room (m)
M momentum (Newton)
$M(U+u)$ momentum obtained from measurements of mean velocity plus S.D. of the velocity fluctuations (N)
$M(p)$ momentum obtained from pressure measurements (N)
p pressure (Pascal)
s co-ordinate along the perimeter of the room (m)
$\underline{u}$ velocity vector (m/s)
U_0 Supply velocity (m/s)
W width of room (m)
(x, y, z) Coordinates

Greek letters
$\Delta = (\partial_x, \partial_y, \partial_z)$ Gradient operator

Subscripts
min minimum
p point
rc rotation centre

1. Introduction

For a frictionless incompressible homogeneous fluid the pressure, p, is determined by the velocity field, u. The pressure field is a solution of the Poison's equation

$$\Delta p = -\rho\nabla\cdot(\underline{u}\cdot\nabla\underline{u}) \tag{1}$$

That is to say, the pressure is a global function of the flow configuration. Thus, it is reasonable to measure the pressure on the room surfaces, and use the results to analyse other properties in the flow field. To the best of the knowledge of the author, this type of pressure measurements have not been done previously.

Miller and Comings [1] reported unique mean static pressure and turbulence measurements in a free jet flow. They questioned the assumption of the mean static pressure gradient in the direction of the jet flow is negligible compared to other mean forces on the fluid. Karimipanah and Sandberg [2] measured the pressure distribution on the walls of a model room with variable lengths and compared with the numerical predictions. They found that in short rooms ($L = H$ and $L = 2H$) the jet arrived at the opposite corner, was deflected at the corner and was constrained to follow the room surfaces. But in the longest model room of their study the jet expanded so it occupied a large fraction of the cross section of the room and the entrainment of air into the jet gave rise to a contra flow in the lower part of the room. Sandberg et al. [3] used the same model room to study the attachment of a buoyant jet to the room surfaces by recording the pressure distribution along the room surfaces.

2. Experimental set-up

A full-scale test room facility with varying room length has been arranged (see Fig. 1). The room width and height

* Corresponding author. Tel.: 0046 26 147800; fax: 0046 26 147803.

S0360-1323/99/$—see front matter
PII: S0360-1323(98)00030-4

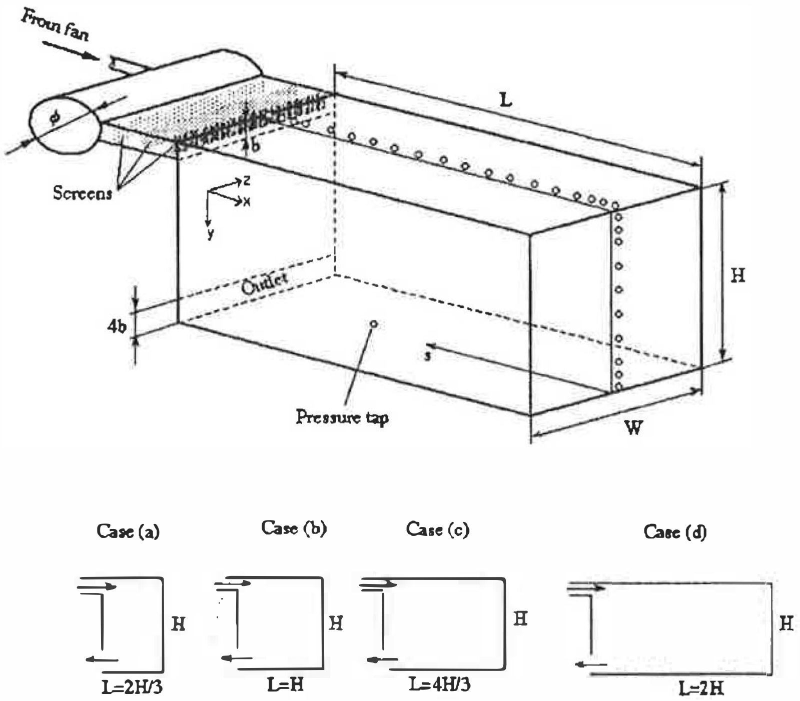

Fig. 1. Experimental facility and definitions.

is $W = H = 3$ m, the room length is varied: $L = 2/3\ H$, $L = H$, $L = 4/3\ H$ and $L = 2H$. The slot height b is 1 cm. The static pressure distribution along the perimeter of the room was recorded via 2 mm diameter holes in the walls. At each point, the time of integration was 5 min and the pressure is refereed to the atmospheric pressure. At the corners, the pressure taps were located closer to each other. The pressure tapping was connected to a Furness micrometer via solenoid vales. The supply velocity was 10.82 m/s for all room sizes.

3. Results and discussion

The pressures were measured for four cases, see Fig. 1. To make comparisons possible between different room lengths the distance s is in Fig. 2 divided by the actual room length L. This means that in terms of s/L the location of (first, second) corner is; Case a (1, 2.5), Case b (1, 2), Case c (1, 1.75) and Case d (1, 1.5). At the first corner, i.e. $s/L = 1$, the pressure levels are very high compared to the other parts of the room and the pressure increases when decreasing the room length. The higher pressure level at the corner of the smaller room is due to the fact that the momentum losses the jet has suffered when arriving at the corner is dependent on the room length. At the second corner (near the floor) one has the same tendency as at the first corner.

3.1. *Impinging region*

As a definition of the point where the influence of the opposing wall starts is taken the location where the pressure starts to increase. The region between the point where the influence of the opposing wall begins and the end of the room we call the 'impingement region'. From Fig. 2 it appears that in the region $0 < s/L < 1.0$ the influence of the opposing wall begins from about $s/L = 0.7$. Although the room length L is varied the impinging jet region occupies the same portion of the room. This is also confirmed by the studies of an axisymmetric jet impinged on a flat plate, e.g., Karimipanah and Sandberg [4].

Figure 3 shows a comparison between the measurements and predicted pressures for the case $L = 2H$. The agreement between predicted and measured values is quite good with respect to the general trend apart from that close at the inlet where there are strong velocity gradients and close to the corners where the velocities are very low. The recirculation bubble at the corner is well captured using an anisotropic version of k–ε turbulence model; see Launder [5] and [6], available in the CFD code FIDAP7.5 [7]. The results in Table 2 obtained for all room lengths were computed using the same turbulence model. Otherwise the location of the rotation centre would have been influenced by the turbulence model used.

3.2. *Jet momentum*

A momentum $M(p)$ has been calculated by integrating the measured pressure the profiles for the different cases in Fig. 1 as

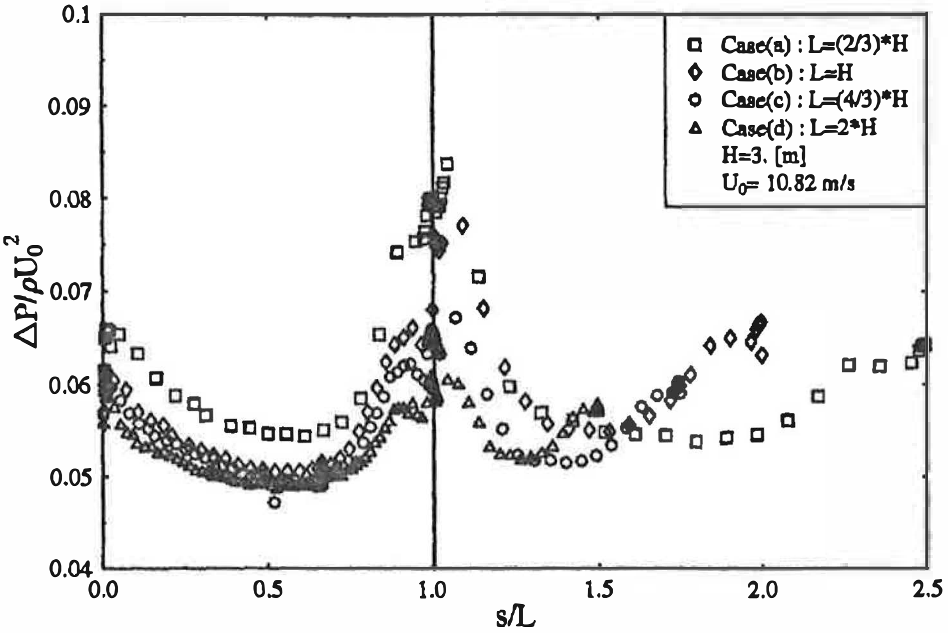

Fig. 2. Pressure measurements for different room sizes. The co-ordinate s covers the ceiling and the wall opposite to the supply.

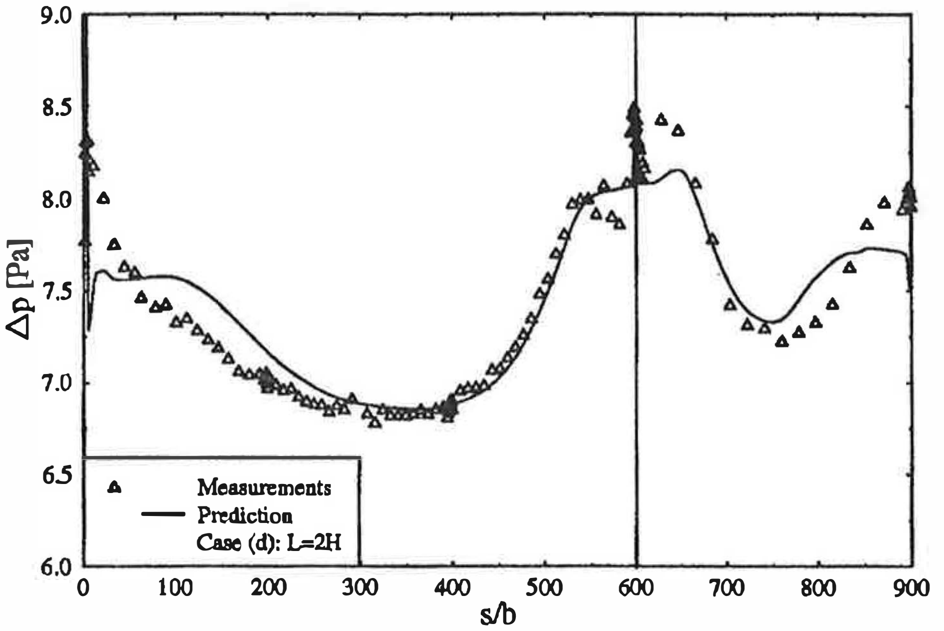

Fig. 3. Comparison of measured and predicted pressures for $L = 2H$ (case (d)).

$$M(p) \cong \int_{s(p_{\min})}^{L} (p(s) - p_{\min}) ds \tag{2}$$

where $s(p_{\min})$ is the point of minimum pressure; see Fig. 2.

$M(p)$ is interpreted as being equivalent to the reaction force at the corner.

Figure 4 shows the jet momentum calculated from the pressure measurements in the impinging region of the different room sizes. For comparison is shown the evolution of the momentum for a jet flowing along a plate by calculating the frictional losses as suggested by Launder and Rodi [8] and the momentum calculated from the velocity measurements in case (d). The results of pressure based momentum, $M(p)$, in Fig. 4, lie above the curve of accepted friction losses except for the case $L = 2H$. The tendency of decreasing $M(p)$ in streamwise direction is due to the increasing room length. With the same inlet Reynolds numbers the jet loses a larger portion of its energy in a longer room compared to a shorter one.

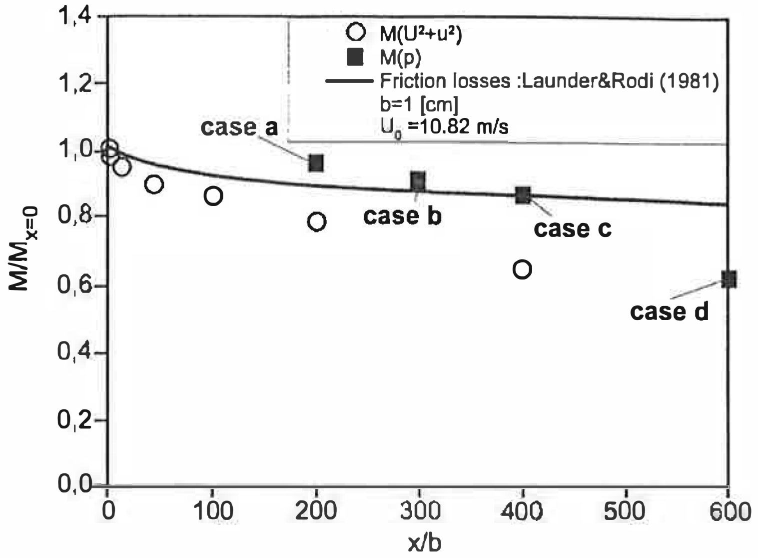

Fig. 4. Comparison of calculated and measured momentum flux in streamwise direction.

3.3. *Minimum pressure and velocity points*

Finding the minimum values of pressure and velocities are of interest when calculating the rotation centre in a ventilated room. The location of the pressure minimum, (see Table 1), was determined from the measured pressure on the ceiling and the wall opposite to the supply air terminal.

The location of minimum velocity points for different room sizes (see Table 2), were calculated from the numerical simulations. It is evident from Tables 1 and 2 that the rotation centre of the air flow pattern in the room is the same using either the simulated flow field or the measured pressures on the room walls. Because of difficulties in velocity measurements in recirculation zones, one can use the simple pressure measurements on the walls to check the validity of the simulations. By using the results of Table 1 or Table 2, the location of the rotation centre (x_{rc}, y_{rc}) can be defined as

$$\left.\begin{aligned} \frac{x_{rc}}{L} &\approx 0.55 \\ \frac{y_{rc}}{H} &\approx 0.53 \end{aligned}\right\} \qquad (3)$$

where L is room length, H is room height x_{rc} is measured from the supply inlet and y_{rc} is measured from the ceiling.

It is worth mentioning that Crommelin [9] used conformal mapping to predict the location of the rotation centre. He used both a full-scale room of

Table 1
Minimum pressure point (results of pressure measurements)

Room length L (m)	Δp_{min} (Pa)	$x_{p_{min}}$ from inlet (m)	$x_{p_{min}}/L$	$y_{p_{min}}$ from ceiling (m)	$y_{p_{min}}/L$	$y_{p_{min}}/H$
$2H$	6.8	3.153	0.525	1.6	0.27	0.53
$4H/3$	6.9	2.075	0.519	1.6	0.40	0.53
H	7.3	1.675	0.558	1.6	0.53	0.53
$2H/3$	7.5	1.225	0.6125	1.6	0.80	0.53

Table 2
Minimum velocity point at rotation centre (results of numerical simulations)

Room length L (m)	U_{min} (m/s)	$x_{U_{min}}$ from inlet (m)	$X_{U_{min}}/L$	$y_{U_{min}}$ from ceiling (m)	$y_{U_{min}}/L$	$y_{U_{min}}/H$
$2H$	0.0023	3.448	0.575	1.50	0.25	0.50
$4H/3$	0.0030	2.163	0.540	1.30	0.32	0.43
H	0.0040	1.5	0.500	1.9	0.65	0.63
$2H/3$	0.0020	1.0	0.500	1.9	0.97	0.63

$V \times H = 5 \times 3.85 \times 3.15$ m and a 5 times smaller scale el, the inlet velocities were 0.5 and 1 m/s. He neg- l the secondary vortices at the room corners and for ull-scale room he found that x_{rc}/L varied between and 0.62 meters and y_{rc}/L was varied between 0.47– n. One can see from Tables 1 and 2 that the results ned by Crommelin are nearly in consort with the s of case (d), i.e., the room with $L = 2H(=6\,\text{m})$. The discrepancies are due to neglecting the influence of r bubbles in Crommelin's studies. The priority of nvestigation over that of Crommelin [9] is that the of the corner recirculating bubbles and room size ncluded.

onclusion

making pressure measurements on the room sur- it has been possible to draw the following con- ons:

e effect of room size on the flow field near the corner pronounced. The pressure level at the corners is ected by room length and this is due to the fact t the momentum losses of the jet increase with the tance the jet has travelled.
e relative location of the point of minimum velocity tation centre) is independent of the room length. empirical relation obtained here may be used for nparison with the numerical results.
changing the position of the wall opposite to the pply, i.e., changing the room length, and measuring ssures on the ceiling and the wall, it is possible to culate the jet momentum flux in the flow direction.
a jet impinges on a wall, which is the case in a slot ntilated room, the impinging region is about 30% room length and this holds independently of room ngth. The deflected flow causes anisotropy of the tur- lent fluctuations. Therefore CFD predictions require the use of a second moment turbulence model to be able to take into account the effect of anisotropy and streamline curvatures at the corner regions.

Acknowledgements

The author would like to thank Hans Allan Löfberg, Head of the Centre for Built Environment, and Professor Mats Sandberg, who initiated this work, for their encouragement and valuable comments. My colleagues, Larry Smids, Claes Blomqvist and Ragnvald Pelttari, who arranged the measuring devices are also gratefully acknowledged.

References

[1] Miller DR, Comings EW. Static pressure distribution in the free turbulent jet. Journal of Fluid Mechanics 1957;3:1–16.

[2] Karimipanah T, Sandberg M. Deflection and influence of room size of a two-dimensional wall jet in a ventilated room. Proc. of the Fourth International Conference on Air Distribution in rooms, ROOMVENT '94, Karakow, Poland, 1994b.

[3] Sandberg M, Wiren B, Claesson L. Attachment of a cold jet to the ceiling-length of recirculation region and separation distance. Proceedings of ROOMVENT'92, Aalborg, Denmark, 1992.

[4] Karimipanah T, Sandberg M. Decay of momentum and velocity in an axisymmetric impinging jet. Proc. of the Fourth International Conference on Air Distribution in Rooms, ROOMVENT '94, Karakow, Poland, 1994a.

[5] Launder B. Lectures in turbulence models for industrial applications. Summer school in Germany, 1993.

[6] Launder B. Turbulence and transition modelling (Lectures). Proceedings of the ERCOFTAC/IUTAM Summer School in Stockholm, 12–20 June, 1995, Ed. Hallbäck M, Johansson AV, Henningson D, Alfredsson HP. Department of Mechanics, Royal Institute of Technology, KTH, Stockholm, Sweden.

[7] FIDAP 7.5. Fluid Dynamics International Inc., 1993.

[8] Launder B. Rodi W. The Turbulent Wall-Jet. Prog. Aerospacw SCI. 1981:19:81–128.

[9] Crommelin RD. Calculations of rotating airflows in spaces by conformal mapping. Energy Conservation in Heating, Cooling and Ventilating Buildings. Vol. 1. CJ Hoogen doorn and NH Afgan, editors, Hemisphere Publishing Corporation.